PORTLAND WESTSIDE LIGHTRAIL CORRIDOR PROJECT WALL 600 MICROPILE RETAINING WALL DESIGN AND CONSTRUCTION

by

Gernot Ueblacker, P.E.
Golder Associates Inc.

ABSTRACT: Reticulated micropile structures have historically been used in slope stabilization applications and consist of a repeating pattern of subvertical pipe piles tied together near grade using a cast-in-place cap or grade beam. Several structures were installed in the United States in the 1970's to stabilize landslides along highways and have met or exceeded the performance expectations. The first micropile structure of this type to be installed in the U.S. Pacific Northwest was designed by Golder Associates Inc (Golder) and was constructed in 1993 under a design build partnering arrangement. Golder has recently participated as the designer and construction consultant on a unique application of micropiling: a micropile structure used as a retaining wall. The structure is currently under construction and serves to support a permanent cut for the approach to the east portal of the Westside Corridor Lightrail tunnel in Portland, Oregon. Cut heights along the retaining wall range from 13 to 30 feet. A typical section of the wall is shown on Fig. 1. The design required consideration of cantilevers attached to the grade beam of up to 13 feet to retain fill required for roadway regrading behind the wall. The design included FLAC finite difference modeling of the service loads to determine structural response of the system to the loading conditions and to calibrate a structural model that accounted for the soil-structure interaction effects to a less sophisticated elastic structural model using STAAD-III. Instrumentation is being procured to monitor the performance of the structure throughout all construction phases.

INTRODUCTION

Micropile structures for use in slope stabilization and earth rention structures have been used in North America since the early 1970's. Golder Associates Inc., (Golder) have pioneered the development of micropile slope stabilization and earth retention structures in the Pacific Northwest. In 1993, Golder participated as the engineer-of-record in a design/build micropile structure that was constructed at the Uptown Apartments in the West Portland Hills in Portland, Oregon. The structure serves to preclude movements of very steep slopes extending west of the apartments and has performed successfully through the recent extremely wet spring. Golder currently has another micropile structure under construction in Portland at the approach the Westside Lightrail East Portal Tunnel - Wall 600. The structure is unique in North America in that it serves as a retaining wall and will receive an architectural cast-in-place facia following excavations made in front of the wall.

The original design of Wall 600 prepared for Tri-Met (owner) by BRW, Inc. included a counterfort concrete retaining wall supported on driven H-piles. Construction of this structure would have required installation of a temporary shoring system to maintain uninterrupted service of Jefferson St. and the

Portand's primary water supply lines. To compress the construction schedule and offer a cost savings to the owner, Golder designed a permanent soil nail wall. The structure was rejected by the City due to concerns for placing permanent ground inclusions in the right-of-way where future utility excavations might damage or disrupt the integrity of the soil nails. As an alternative, Golder proposed a permanent micropile wall that could be kept within the envelop of the original counterfort structure as shown on Fig. 1. The City accepted this alternative provided that the structure could be maintained outside of a potential future utility construction zone as shown on Fig. 2. Subsequently, design on the structure was initiated in January of 1996 and, to compress certain phases of the construction schedule, the design had to be completed in two to three weeks.

PROJECT DESCRIPTION

Wall 600 extends from the east end of the Westside Lightrail cut and cover tunnel at the east portal (EB LRT STA. 936+50) approximately 600 feet to just beneath the Vista Avenue Bridge (EB LRT STA. 941+74). The alignment generally parallels the south side of Southwest Canyon Road where it meets Jefferson Street. The final excavation will be extended approximately 5 feet below the top of rail to allow installation of railway ballast material. Including the railway ballast overexcavation, the wall heights vary between 30 feet in the vicinity of the cut and cover structure and 13 feet in the vicinity of the Vista Avenue Bridge. The total wall area will approach 12,150 square feet.

Wall 600 is considered a life-line structure. The primary function of Wall 600 is to accommodate a grade change between the rail alignment and the alignment Jefferson Street thus maintaining uninterrupted service of the rail and road traffic. The secondary purpose of Wall 600 is to provide support for existing utilities. These include two 30-inch and two 36-inch water mains - the primary water supply lines servicing the downtown Portland area.

SYSTEM DESCRIPTION

The permanent micropile wall consists of 7 5/8-inch API N80 pipe piles fully grouted and reinforced with an epoxy-coated #10 to #14 ASTM 615 (Grade 75) deformed bar and is shown on Fig. 1. API N80 is the conventional material used for micropile and pin pile installations in North America. The micropiles are installed at varying vertical and subvertical angles within the envelop of the owner-designed counterfort wall. The system consists of either a 5 or 10-foot bents of two vertical (compression) and two battered (tension) micropiles as shown in Fig. 4. The subvertical micropiles are generally installed at an inboard angle of 30 degrees throughout the majority of the alignment. However, toward the eastern

end of the alignment this inclination steepens to maintain the geometric configuration required by the city for protection of future utility installation as shown in Fig. 2. The City required that no micropiles encroach within about 12 feet of the finish grade at the curb line.

Micropiles are tied together at existing grade with a grade or cap beam designed to service the shear and torsion loads imposed by the tension and compression micropiles (Fig _). A temporary shotcrete facing approximately 4-inchs thick reinforced with #5 deformed bars 12-inches on center is applied during excavation. The final facia consists of a reinforced concrete section 12-inches wide with two curtains of deformed reinforcing bar as shown in Fig. 3. In areas, the final facia will cantilever above the grade beam up to 13 feet.

CONSTRUCTION SEQUENCE

Site preparation included clearing and grubbing, removal of an abandon 36-inch steel pipe and excavation for the grade beam. Pile installation was then initiated with the in-board vertical micropiles installed first followed by battered tension piles and out-board vertical micropiles. The tops of all piles are surveyed to ensure compliance with the embedment tolerances. Pile installation was preceded by a conducting a series of six compression and six tension pile verification tests.

Excavation in front of the wall has not yet been initiated but will be staged in approximately 6 foot lifts. During excavation, shotcrete will applied to the excavation face to temporarily prevent facial raveling. Connection to the micropiles will be via head studs welded to the front line micropiles. Following completion of the excavation, a leveling pad will be poured to allow erection of the one-sided forms. A cast-in-place (CIP) concrete facia will then be constructed. Connection of the micropile structure to the CIP facia will also be made using headed studs welded to the micropiles and embedded in the cast-in-place grade beam. and facia as shown in Fig. 3.

SUBSURFACE CONDITIONS

Our primary field investigation was conducted on March 30 and 31, 1995, and consisted of drilling two borings and excavating four test pits. Test pits were excavated using a rubber-tired backhoe to a depth of 7.5 to 9 feet. The test pits were left open for approximately 24 hours to observe stand up characteristics of the sidewalls. No samples were taken from the test pits.

Two borings were drilled to depths of 39 and 30 feet, respectively. The drilling was conducted using a mobile B-61 truck-mounted drill utilizing 4-inch inside diameter, hollow-stem auger. During the drilling operation, disturbed, but representative, soil samples were obtained at 5-foot intervals or as directed by the engineer. The samples were obtained in accordance with the Standard Penetration Test procedure as described in ASTM D-1586. In addition, where soil conditions allowed, undisturbed samples were obtained using a 30-inch Shelby tube sampler. Groundwater levels were measured by reading water levels in the borings at the conclusion of drilling.

Based on the information obtained from in our explorations, the subsurface conditions are composed of a sequence of soil units and rock including fill, alluvium and weathered basalt. Each of these soil and rock units are described below.

- Fill - Soft to stiff fill was encountered at the surface in all our explorations. The fill thickness was about 25 to 21 feet and consisted of soft to stiff, silt with some sand and gravel. The test pits and nail installation logs indicate scattered basalt rubble ranging in size from fine gravels to cobbles.

- Alluvium - One boring encountered a firm or loose alluvium unit underlying the fill consisting of stratified, silt with little fine sand. This unit has been interpreted as a recent alluvial deposit.

- Basalt - This weathered bedrock unit was encountered in one boring at a depth of 24.5 feet. Borings conducted by others also encountered bedrock. The bedrock consists of very hard, weathered to slightly weathered Basalt.

Test pit explorations were excavated predominantly in silt fill. No caving or seepage was observed in the test pits. The test pits were originally conducted to obtain an indication of the stand-up time characteristics for construction of the soil nail wall alternative but also serve the same function for the micropile wall excavation phase.

Groundwater levels were measured in the borings at the time of drilling. The groundwater depths are below the bottom of the micropile wall excavation at 30 and 28 feet, respectively.

LABORATORY TESTING

Disturbed and undisturbed samples from the drilling performed on March 31, 1995 were returned to our soils laboratory in Seattle and submitted for testing. A consolidated - undrained (CU) 3-stage triaxial

compression test was performed on an undisturbed Shelby tube sample. Strength testing results are summarized below:

TABLE 1

STRENGTH PROPERTIES

Application	Friction (Deg)	Cohesion (Psf)	Unit Weight (Pcf)
Test Results	32	300	113.5

The laboratory strength testing was used as a basis for developing the design earth pressure in conjunction with engineering judgment, observations of adjacent excavations during installation of the water mains and the owners previous design criteria. A cohesion strength component of 200 psf was considered in developing the design earth pressure.

DESIGN APPROACH

The structure was designed using conventional earth pressure diagram, developed from previously established project design criteria by the Owner's engineer. This approach was used since it was familiar to the regulators and reviewers of the structure. Since the design of a micropile retaining wall such as Wall 600 was unprecedented in the available literature, an approach using a simplified earth pressure diagram but verified by more sophisticated finite difference modeling was deemed appropriate. The simplified loading diagram is shown on Fig. 6 and discussed further below. The design of the structure was performed using STAAD-III. All elements of the system were incorporated into the STAAD-III model and 25 % of the earth pressures shown in the loading diagram were applied to each of the four micropiles per bent. The load pressure distribution assumption was substantiated using a FLAC finite difference model that would provide a more reliable estimate of the soil-structure interaction effect not captured by STAAD-III.

LATERAL EARTH PRESSURE DIAGRAM

Using the design strength parameters of $\varnothing' = 30^{o}$ and $c' = 200$ psf we determined the theoretical earth pressure diagram and modified this diagram in accordance with the alternative procedures recommend by Bowles (1988). The theoretical earth pressure diagram calculations were performed for a typical 25-foot cut. Using the alternative earth pressure diagram approach recommended by Bowles, we calculated an

equivalent fluid density of 28.8 pounds per cubic foot (pcf). Our design was, therefore, based on an equivalent fluid density of 30 pcf.

As discussed below we reduced the potential hydrostatic pressure in consideration of the vertical drainage behind the wall. Therefore, we conservatively decided not to reduce the equivalent fluid density below the water table in consideration of buoyant weight.

WATER LINE SEEPAGE FORCES

The City of Portland requested that the design include consideration of hydrostatic forces imposed due to potential rupture of the recently installed 30-inch water lines. The design considers a simplified method of determining the seepage force as presented by R. E. Hunt (1986) Geotechnical Techniques and Practices. The proposed method determines the seepage forces acting on a failure plain considering the equipotential lines developed behind a wall with a vertical drain. The approximate angle of the failure plane is derived from FLAC analyses. Interpretation of the FLAC, indicate that the active state of the soil is mobilized and the micropile reinforcing elements are engaged when the failure plane assumes approximately a 45^{o} angle with the vertical.

Using this failure angle and the methods proposed by Hunt (1986) we have determined that the seepage force on the system is parabolic but simplified to be uniform in our design. Although the orientation of this seepage force is perpendicular to the failure plane, the design conservatively considers the full magnitude to be horizontal.

IMPACT LOAD

In accordance with the design requirements for the counterfort structure, a vehicle collision load of 10 kips on the upper parapet was included in the design. This is consistent with the recommendations of the 15th Edition of the AASHTO Bridge Design Specifications. The impact load is considered to be an extreme event that is not coincident with other extreme events in accordance with the AASHTO LRFD specification. The impact load is distributed over a 5-foot width on the parapet in accordance with the requirements of the AASHTO Bridge Design Specifications.

TRAFFIC SURCHARGE

The project design criteria established by the owner required the design to include a uniform vertical traffic/construction surcharge of 600 psf. The surcharge was modeled as a uniform earth pressure and

was multiplied by an active earth pressure coefficient of Ka =0.33 to yield a horizontal component of 200 psf.

SEISMIC DESIGN CONSIDERATIONS

The seismic loading conditions for the micropile wall were dictated by Section 2.11 Seismic Design, of the report entitled Design Criteria, West Side Corridor Project, Portland, Oregon prepared by the owner's engineer dated June 1993. Table 2 summarizes the design earthquake parameters for the operating design earthquake (ODE) and the maximum design earthquake (MDE). The peak acceleration, velocities, and displacements included in this table have been reproduced below in Table 2.

TABLE 2

DESIGN GROUND MOTION PARAMETERS

DESIGN EARTHQUAKE	DESIGN GROUND MOTION PARAMETERS IN ROCK					
	Peak Acceleration (g)		Peak Velocity (ft/sec)		Peak Displacement (ft)	
	Horiz.	Vert.	Horiz.	Vert.	Horiz.	Vert.
ODE	0.20	0.13	0.53	0.35	0.30	0.20
MDE	0.30	0.20	0.80	0.53	0.40	0.30

The Mononobe-Okabe approach was used in estimating the seismic soil pressures on the micropile retaining structure. Given the close proximity to rock, the peak accelerations indicated in Table 2 were used in determining the horizontal and vertical seismic coefficients. The horizontal coefficient was determined in accordance with the following equation conventionally used in seismic design of retaining walls for an allowable deformation (d) of two inches:

Where, $K_H = 0.67(A)(A/d)^{1/4}$

A = See Table 2 for peak acceleration

d = 2.0 inch

and, $K_V = 2/3\ K_H$

(Ref. ASCE Geotechnical Journal, Vol. 105 GT4, 1979 pp 449-464).

The ratio of 2/3 between the vertical and horizontal seismic coefficients indicated in Table 2 was maintained in determining the seismic lateral earth pressures.

The horizontal and vertical seismic coefficients and lateral earth pressures for the ODE and MDE seismic loading conditions estimated based on the Mononabe-Okabe equations are shown on Table 3.

TABLE 3

SEISMIC DESIGN CRITERIA

DESIGN CONDITION	K_H (g)	K_V (g)	UNIFORM SEISMIC LATERAL EARTH PRESSURE (psf)
ODE	0.08	0.05	4.6H
MCE	0.13	0.08	8.8H

STAAD-III LFRD ANALYSES

The load factor combinations were developed considering both the project design criteria document noted earlier and the 15th addition of AASHTO and the first edition of the AASHTO LRFD bridge design specifications. The load factors and combinations of loads are shown in Table 4 and were predominantly used in the STAAD-III computations. In accordance with the AASHTO LRFD design guidelines the impact load (C_T) is considered an extreme event and was isolated from the other extreme events. The water pressure force (B) is postulated due to a rupture of the water line. Such a rupture would be detected and repaired shortly, therefore, this load was also considered an extreme event independent of other extreme events.

TABLE 4

LOAD FACTOR COMBINATIONS

Group	E	B	C_T	ODE	MDE
I	1.69	-	-	-	-
VII_{CT}	1.69	-	1.3	-	-
VII_{ODE}	1.69	-	-	1.3	-
VII_{MDE}	1.3	-	-	-	1
VII_B	1.69	1.3	-	-	-

E = Earth pressure (includes traffic surcharge)
B = Water pressure
C_T = Impact Load
ODE = Operating Design Earthquake
MDE = Maximum Design Earthquake

The micropile structure was analyzed using STAAD-III at six sections for the five cases indicated in Table 4. Additionally, a service load condition equivalent to a Group I analyses without load factors was analyzed to verify the service load deflections and loads of the structure and to provide a basis of comparison to the FLAC analyses. As noted above, all loads on the piles were distributed uniformly

between each of the four piles per bent. With the exception of earth pressure, all loads were modeled as uniform pressures. Earth pressures due to the soil were modeled in a hydrostatic manner as shown on Fig. 6.

FLAC ANALYSIS

LRFD analyses of the micropile structure were performed for a service load and four extreme event loads as shown on Table 4. The LRFD analyses were conducted using the structural design software STAAD-III by applying the earth pressure diagram equally over the four piles in each typical bent. To verify the earth pressure distribution assumption and because STAAD could not accurately model the soil/structure interaction effects we performed more rigorous finite difference analyses for service load conditions using FLAC. The finite difference model is shown on Fig. 7. The FLAC model was used as a "baseline" to verify the conservatism incorporated in the STAAD-III model and the assumed load distribution. The results of the comparison are shown on Fig. 8 and demonstrate that for most elements of the system the STAAD-III model was adequate and conservative.

The soil and rock parameters that were used in the FLAC analysis were slightly conservative best estimates based on the overall nature of the site. The variability of these parameters was evaluated by reducing the selected strength parameters, stiffnesses, and moduli by 20 percent. This changed the FLAC results only slightly. The overall magnitude of the results were about the same. Given the conservative nature of the STAAD-III model when compared to the FLAC model, the results were still deemed acceptable. Naturally, it would have been advantageous to perform parametric analyses with FLAC but that was economically prohibitive. The level of analysis that was performed is viewed as adequate.

The uncracked or gross moments of inertia for the grade beam, CIP wall, and shotcrete facing, were used in the FLAC service load analysis. The moments that developed on the elements are significantly less than the corresponding cracking moments. This is as expected given that the cracking moment is typically on the same order as the yield moment for sections as lightly reinforced as these.

For tension piles, the grout was used in the axial stiffness calculation above the grout zone. In a relatively short distance (on order of 5 feet) from the base of the pile, the axial load was transferred to the entire section as the pipe, grout, and bar were stretched, and bond stress developed between the three elements. At service load levels, the resultant tensile strains were actually below the grout cracking strain. For both tension and compression piles, the transformed areas were used in terms of a steel

modulus (only 25.8 in^2 / 8 = 3.22 in^2 was used for the grout). A supplemental factored analysis using cracked grout sections had negligible effects on the results.

SLENDERNESS AND STABILITY

SERVICE LOAD ANALYSES

Most micropile structures are fully embedded and, therefore, slenderness and buckling of the micropiles is irrelevant. However, the construction of Wall 600 required that the front line micropiles be fully exposed. The difficulty in assessing slenderness effects is in determining the effective length (KL) for the analyses. Design relationships presented by the AASHTO or AISC specifications that check axial load and flexure interaction and slenderness effects require input parameters for effective length and end restraint. However, the piles are not idealized column elements as in a building or the column piers of a bridge where the end restraint and effective length are relatively well defined. Because the end restraint and lateral support provided to the piles involves complicated soil-structure interaction, simplified approximations will only result in overly-conservative results that produce designs that are economically prohibitive. FLAC provides a more accurate model for the pile behavior. Axial and flexural yield levels are provided to FLAC, and the soil, shotcrete and CIP lateral support are directly modeled. As lateral and axial load develop on the piles in FLAC, the p-D effect is computed and the lateral stability is directly a function of the soil support.

For the FLAC analysis of Panel 3 (the panel with the highest cantilever), at the excavation stage and at the final stage of construction, the pile stresses due to the service loading caused by self weight of the retained ground are indicated in the following table:

TABLE 5

PANEL 3 SERVICE LOAD STRESSES

Construction Stage	Pile Axial Compression (k)	Pile Moment (k-in)	Pile Area (in^2)	Pile Section Modulus (in^3)	Pile Axial Stress (ksi)	Pile Flexural Stress (ksi)	Pile Combined Stress (ksi)
Prior to CIP Wall	9.03	160	10.0	14.9	0.90	10.7	11.6
Final	35.4	149	10.0	14.9	3.54	10.0	13.5
	17.9	204	10.0	14.9	1.79	13.7	15.5

In view of the relatively low stresses (by comparison to the yield stress of 80 ksi) indicated above, the lateral stability was considered acceptable and not a potential problem. However, design team members

reviewing the design requested a more rigorous analysis. Our approach consisted of verifying the ability of FLAC to capture the Euler bulking load on a simple member, developing the FLAC axial/bending stress interaction diagram and performing a factored analysis for the governing load condition in Table 4 on Panel 3.

EULER BUCKLING LOAD VERIFICATION

Prior to performing additional analyses of the micropile structure, we investigated the capability of FLAC to capture the buckling phenomenon. A simple analysis model of a beam-column was considered. The model and the analyses results are shown on Fig. 9. The model consisted of a 15-ft long pipe pinned at each end. The pipe properties were identical to the 7-inch diameter API N80 pipe used throughout the design of the micropile structure. With pin-supports, the effective length of the pipe was KL = 15 ft. Identical axial load and moment were applied at each end of the pipe. The ratio of the end moment to the axial load is defined as the initial eccentricity, $e_i = M_i / P$. FLAC may be run in small-strain and large-strain mode. Although both were examined, only the results in large-strain mode will be discussed here. The main variables of interest in the FLAC analyses were the axial load (P), the initial eccentricity (e_i), and the plastic moment capacity of the pipe (M_P).

The pipe has a radius of gyration, r = 0.188 ft (Appendix A). Therefore, the slenderness ratio of interest is KL/r = 15/0.188 = 79.8. For this value of KL/r and the pipe values for modulus and area, the Euler buckling load is computed to be 450.5 kips. This is 56.3% of the yield load of 800.0 kips. Note that AASHTO(1992) Equation 10-151 for the inelastic buckling strength of this member indicates 444.0 kips or 55.5% of the yield load. Therefore, the elastic Euler value is essentially identical to that based on the inelastic equation in AASHTO(1992).

The FLAC results shown on Fig. 9 are as follows. For zero eccentricity, FLAC indicates that axial load may be applied indefinitely with no buckling. However, for even the slightest eccentricity (say $e_i = 0.01$ ft which will be the case in the micropile wall analysis), FLAC predicts buckling to occur just below the Euler load. As the initial eccentricity is increased to $e_i = 0.1$ ft, the buckling load decreases due to the p-Δ effect. Sensitivity analyses were conducted for both infinitely large plastic moments and the theoretical plastic moment of $M_p = 135$ kip-ft. If the theoretical plastic moment capacity is considered, FLAC predicts the buckling load will decrease even more but the results do not appear to be extremely sensitive to this value.

It should be noted that FLAC does not look at the combined stress due axial load and moment. That is, if the plastic moment capacity has not been reached and buckling has not occurred, the combined stresses due to the axial load and the maximum moment may still exceed the yield stress. Buckling would occur at

the yield stress in practice. For large enough initial eccentricities (say 0.1 ft), if the buckling or failure load in FLAC is considered to be that which causes either outright buckling or a combined stress equal to the yield stress, then FLAC will predict interaction relationships such as those shown on Fig. 10 depending on the initial eccentricity.

The interaction relationships for small eccentricities are reasonably similar to published relationships in codes that address combined loading and slenderness. The eccentricities of the micropile system predicted by FLAC are judged to be sufficiently prevalent such that simple comparison of the maximum combined stress due to moment and axial load to the yield stress of members should result in a reasonable prediction of the adequacy of the design.

FACTORED ANALYSES OF PANEL #3

In order to investigate the FLAC model response at the factored load or ultimate state, a factored load analysis was performed for the previously developed model of Panel #3 (highest cantilever) for the vehicular impact load combination. The vehicular impact load combination was selected because it often governed in the STAAD-III analyses and because it was the most straightforward to consider in the FLAC model.

The structural properties for the FLAC model were changed from the service load analysis model based on review comments issued by the design team and based on the inherent differences between the service and extreme event load conditions. In brief, the grout annulus was considered cracked and was therefore ignored for the pile axial and bending stiffness; a #14 bar was used in the micropile rather than a #10 bar; the shotcrete reinforcement was modified to #5's @ 12" each way; and, only the fully-cracked flexural stiffness were used for both the shotcrete wall and the CIP wall and footing. These modifications are not judged to significantly effect previous analyses.

In order to consider factored loads, the unit weight of all soil and rock materials was increased by a factor of 1.69. The surcharge loading of 600 psf was actually applied as a 600(1.69) = 1014 psf surcharge behind the wall. The vehicular impact load of 10 kips was factored by 1.3 and applied at the top of the 3-ft parapet. This 13 kip load was considered to be distributed over a width of 29 (at the grade beam feet) so that only 448 plf was actually applied in the model. The 29 feet is based on a 5-ft load width at the top of the cantilever, which is distributed to the level of the grade beam at a 45 degree angle on either side in accordance with AASHTO. With the top of the cantilever extending 12 feet above the grade beam centerline, this results in an equivalent load width at the level of the grade beam of 2(12) + 5 = 29 ft for use in the two-dimensional FLAC model.

As in the previous FLAC analyses, all soil and rock materials were modeled as elasto-plastic Mohr-Coulomb materials with slightly conservative, best-estimate stiffnesses and strength properties. The piles were defined to interact with the soil and rock grid through standard lateral pile reaction springs and conservatively selected axial pile spring stiffnesses and strengths.

Two stages of the excavation were considered in analyses: (1) the final excavation stage prior to completing the shotcrete and, (2) the final wall configuration with backfill placed and subject to the impact load. The results are shown on Fig. 11 - 19 and discussed further below. A summary of selected analysis results from all of the FLAC analyses performed in this supplemental study is shown on Fig. 20

FACTORED LOAD ANALYSIS: END OF EXCAVATION

After initialization of the existing slope geometry, installation of the grade beam, installation of the micropile system, and sequenced excavation and construction of the shotcrete facing were modeled in FLAC. Selected analysis plots are shown on Fig 11 and 12. Fig. 11 shows an exaggerated deflected shape of the micropile structure. Fig. 12 illustrate the displacement vectors.

Maximum pile moments and axial loads are tabulated in Fig. 20. Again, it is of interest that the maximum pile axial load occurs for the back row vertical micropiles (Pile 2) and is about 60 kips with the maximum moment of about 20 k-ft. The maximum combined stress ratio is not shown but is computed as in 0.22. Therefore, even at the factored state for this stage of construction, the maximum pile stress is only about 20% of yield for this construction stage. Maximum lateral deflections are on the order of 0.1 ft. The maximum factored deflections are considered relevant only from the perspective that sufficient eccentricity is one condition for FLAC to model the buckling behavior adequately under additional axial load. Also, since the analysis is influenced by factored unit weights, deflections are not considered representative of service load deflections.

FACTORED LOAD ANALYSES: FINAL CONFIGURATION

After casting the footing, attachment of the CIP to the headed studs, and construction of the cantilever, the placement of backfill behind the cantilever was modeled in three stages. With the backfill in place, the surcharge load was first added, and the vehicular impact load was finally applied to the top of the cantilever. Selected analysis plots are shown on Fig.'s 16 and 17. Fig. 16 shows an exaggerated deflected shape of the micropile structure at the final load conditional under the factored weights. Fig. 17 shows the displacement vectors.

Maximum pile moments and axial loads are tabulated on Fig. 20 . Again, it is of interest that the maximum pile axial load again occurs in Pile 2 and is about 143 kips and the maximum moment is about 50 k-ft. The maximum combined stress ratio as computed in the table is 0.47. Therefore, even at the factored state, there appears to be significant reserve capacity in the piles for the final configuration. Maximum lateral deflections under the factored unit weights are on the order of 0.3 ft. The maximum factored deflections are considered relevant only from the perspective that sufficient eccentricity is one condition for FLAC to model the buckling behavior adequately under additional axial load. As indicated on Fig. 8 the maximum deflections under the service load conditions based on the FLAC analysis for this panel are 0.076 ft.

RESERVE PILE AXIAL CAPACITIES

In order to investigate the potential reserve buckling capacity available in the front row of micropiles, an additional concentrated load was applied to the grade beam directly above the front pile line. This was carried out at the deformed configurations at the two construction stages considered above. The exaggerated shapes of the micropile system at the failure condition are shown on the FLAC plots in Fig's 13 and 18. The mode of failure for both excavation stages was punching failure of the front line micropiles followed by development of a plastic hinge at the grade beam as shown on Fig. 14.

END OF CONSTRUCTION STAGE

For the case prior to CIP wall placement, the concentrated load was increased from 0 to 200 k/ft in 20 to 50 k/ft increments. The lateral deflections of the first pile line at the level of the grade beam, at the location of the maximum deflection, and at the wall base are shown on Fig. 20 along with the maximum axial loads and moments in the piles. A plot of the axial load versus grade beam lateral deflection response for Pile 1 is shown on Fig. 15. Throughout loading, the front row micropile (Pile 1) was bent in double curvature, significantly reducing the effective length governing lateral stability. When the 200 k/ft load was applied, Pile 1 reached an axial load of over 600 kips and punched through the soil and rock. The punching resulted in plastic hinges developing at the tops of the piles near the grade beam and the lateral deflection at the grade beam increased significantly. Equilibrium was never achieved under this load in FLAC. It is important to note that the maximum combined pile stresses exceeded the yield stress in FLAC before punching through the soil and in practice buckling could likely have occurred at the yield stresses. FLAC plots in Fig. 13 show the deflected shapes of the micropile structure at the 200 k/ft load level.

In summary, the observed response for additional axial load at this construction stage was that the pile structural capacity was achieved without outright buckling in FLAC. Because the combined stress is not considered by FLAC, the axial load in Pile 1 was taken even higher until it was limited by punching in the grout zone. Because the effective length due to double curvature of the pile is much less than the distance from the grade beam to the wall base, the pile buckling load predicted by FLAC exceeds the yield capacity of the piles. (FLAC would likely predict the Euler load or less which would likely well exceed the pile structural capacity for effective lengths on the order of 5 to 10 ft.) Actual pile buckling would likely accompany the development of the yield stress on the pipe, which corresponded to an added load of about 110 k/ft to the grade beam based on the combined stress ratios determined from the FLAC analysis.

FINAL CONFIGURATION STAGE

For the final configuration, the concentrated load was increased from 0 to 200 k/ft in 50 k/ft increments. The lateral deflections of the first pile line at the level of the grade beam, at the location of the maximum deflection, and at the wall base are also tabulated in Fig. 20 along with the maximum axial loads and moments in the piles. A plot of the axial load versus grade beam lateral deflection response for Pile 1 is shown on Fig. 19. Throughout loading, Pile 1 was bent in double curvature, significantly reducing the potential effective length in terms of lateral. When the 200 k/ft load was applied, Pile 1 reached an axial load of nearly 600 kips, and as with the previous stage, punched through the soil and rock. The punching resulted in plastic hinges developing at the tops of the piles near the grade beam and the lateral deflection at the grade beam increased significantly (Fig. 18). Note that the maximum combined pile stress just exceeded the yield level in FLAC at the 100 k/ft load level. In reality, pile buckling would likely accompany the development of the yield stress on the pipe.

LOAD LOCATION SENSITIVITY

To investigate the sensitivity of model to location of the axial load we conducted an analyses with the additional axial load aligned over the center of the grade beam for the final configuration. The cantilever load was imposing slight double curvature in the piles initially. However, as additional axial load was applied single curvature developed. At approximately 250 k/ft. the yield stress in the pile was reached due to combined axial and flexural stresses. Axial loads in each vertical pile were about 550 kips at this level or about 400 percent greater than the largest initial vertical load of 142 kips.

CONCLUSION

The supplemental analyses demonstrated the reserve capacity of the structure was adequate to preclude concerns for buckling or slenderness instability. The analyses also demonstrates that it is necessary to model all components of the system (including soil/`structure interaction) in determining the effective lengths of the front line micropiles. Although some may consider our analyses outside the conventional practices of structural engineering, we feel we have brought to bear the most sophisticated analyses in evaluating the performance of this highly complex structure. Through more rigorous analyses we demonstrated that soil/structure interaction effects produced a more stable configuration in the reticulated micropile structure than might have been conventionally assumed. This resulted in a more economical but equally reliable structure and ultimately time and cost savings to the Owner.

ACKNOWLEDGMENT

The author would like to recognize first and foremost our client Frontier/Traylor : A Tri-Met Joint Venture and the owner Tri-Met, for without open-mined clients and owners opportunities like Wall 600 remain dreams. The author is also extremely grateful Mr. John Critchfield formerly of Parsons-Brinkerhoff , the owners engineer, who's support, encouragement and persistence ultimately led to the successful permitting of the project. The author also extends a debt of gratitude to staff of Golder Associates Inc. who persevered a formidable design schedule, in particular, Dr. Chris Wolschlag, project engineer with Golder, who did the "heavy lifting" by performing all the FLAC and STAAD-III analyses.

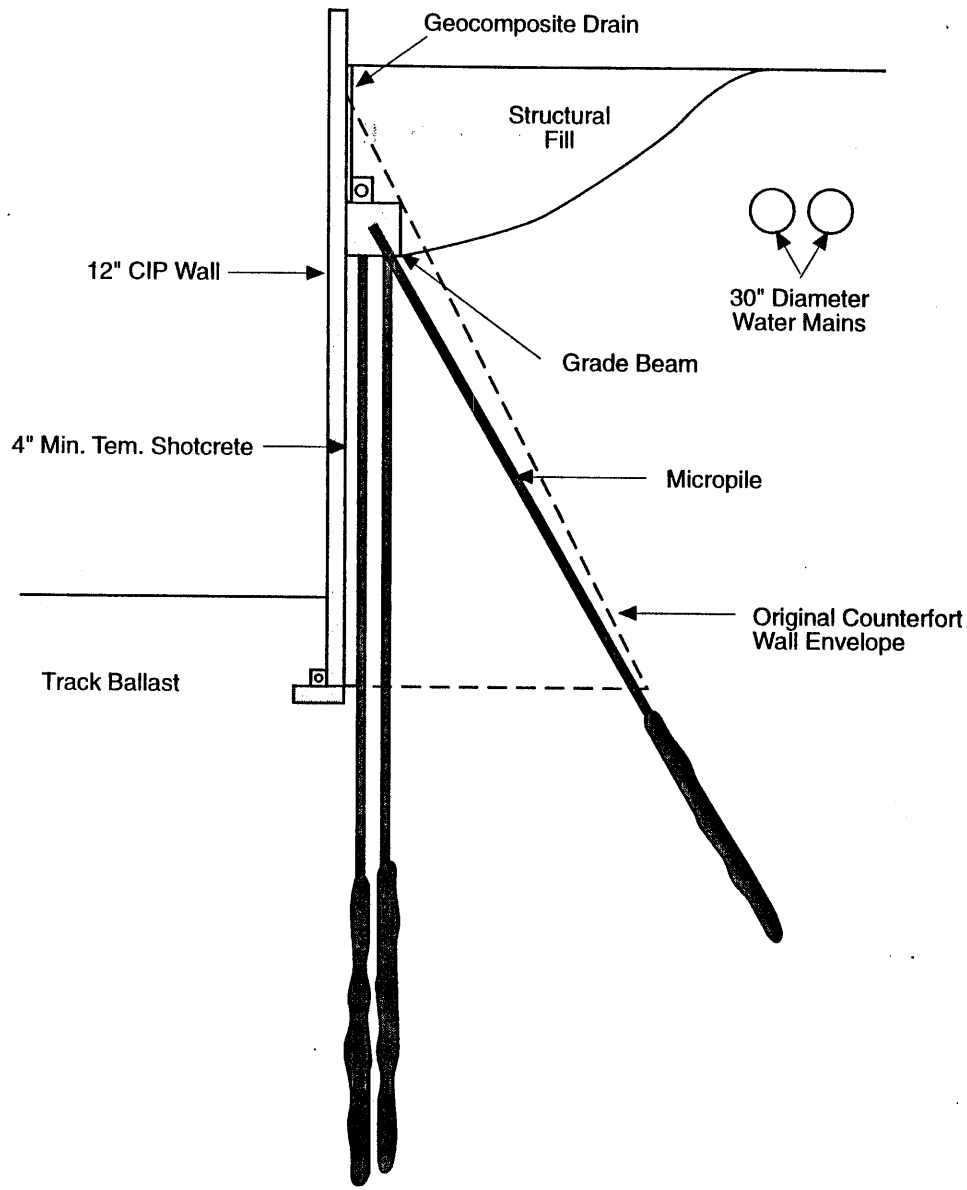

FIGURE 1
TYPICAL WALL SECTION
WALL 600/PRESENTATION/CO

PROJECT NO. IP3 2572 DRAWING NO. 66759 DATE 5/31/96 DRAWN BY EA

Golder Associates

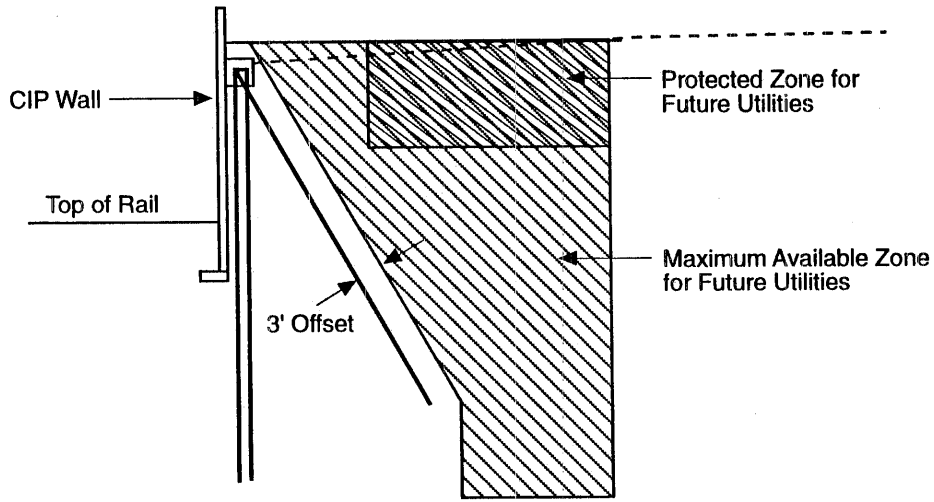

FIGURE **2**
UTILITY PROTECTION
WALL 600/PRESENTATION/CO

PROJECT NO. IP3 2572 DRAWING NO. 66760 DATE 5/31/96 DRAWN BY EA

Golder Associates

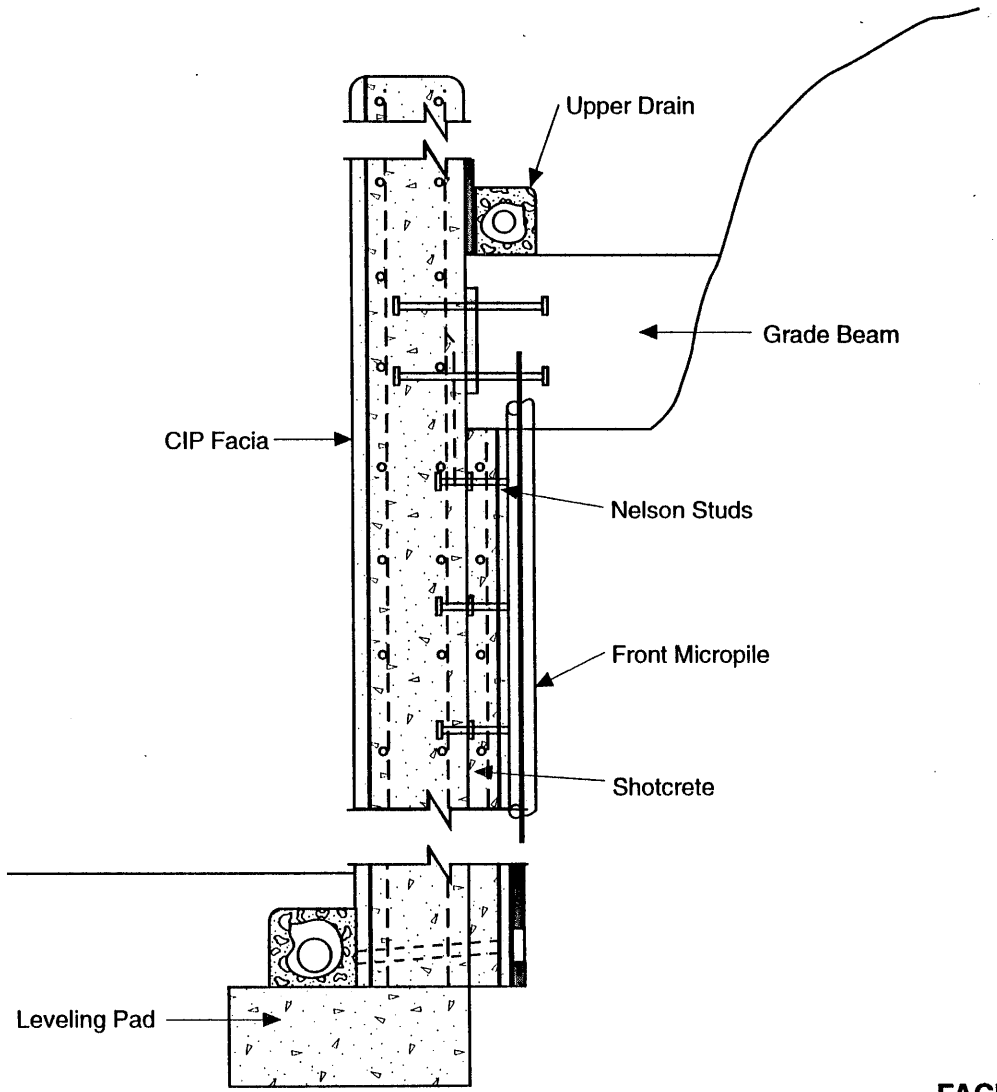

FIGURE **3**
FACING CONNECTION WALL SECTION DETAIL
WALL 600/PRESENTATION/CO

PROJECT NO. IP3 2572 DRAWING NO. 66753 DATE 5/31/96 DRAWN BY EA

Golder Associates

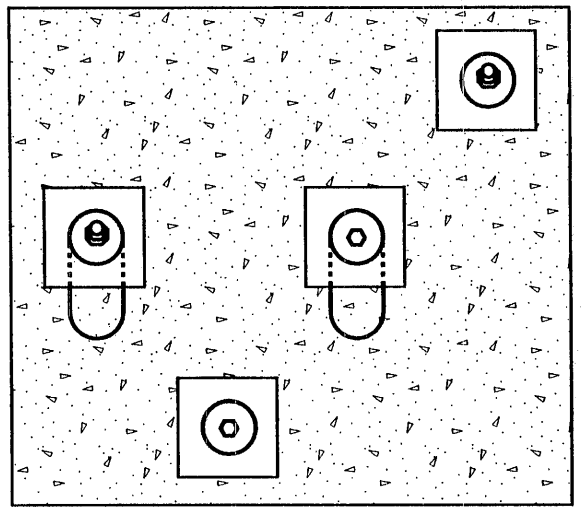

Pile Spacing Schedule

Panel No.	Pile Spacing
1-10	1' - 3'
11-17	2' - 6'

FIGURE **4**

TYPICAL MICROPILE BENT

WALL 600/PRESENTATION/CO

PROJECT NO. IP3 2572 DRAWING NO. 66758 DATE 5/31/96 DRAWN BY EA

Golder Associates

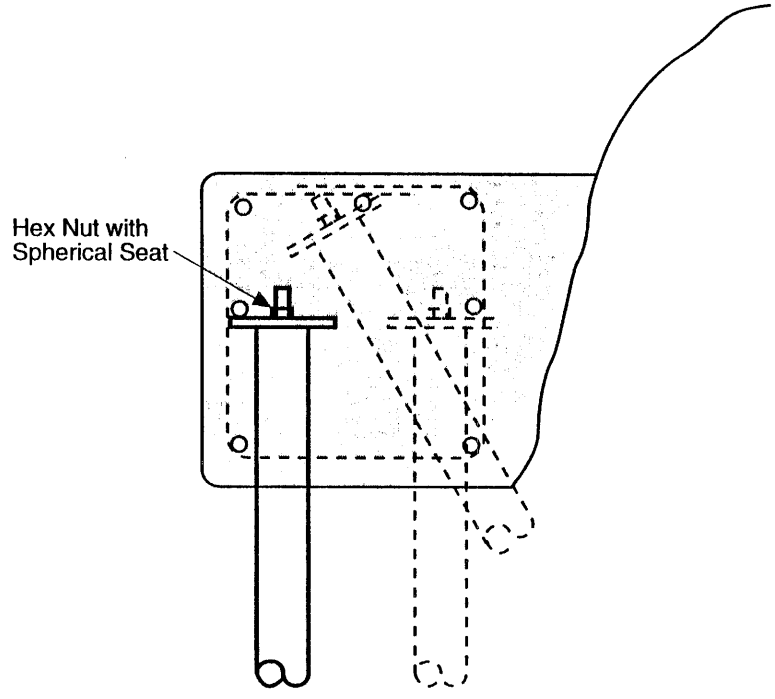

FIGURE **5**

GRADE BEAM DETAIL

WALL 600/PRESENTATION/CO

PROJECT NO. IP3 2572 DRAWING NO. 66757 DATE 5/31/96 DRAWN BY EA

Golder Associates

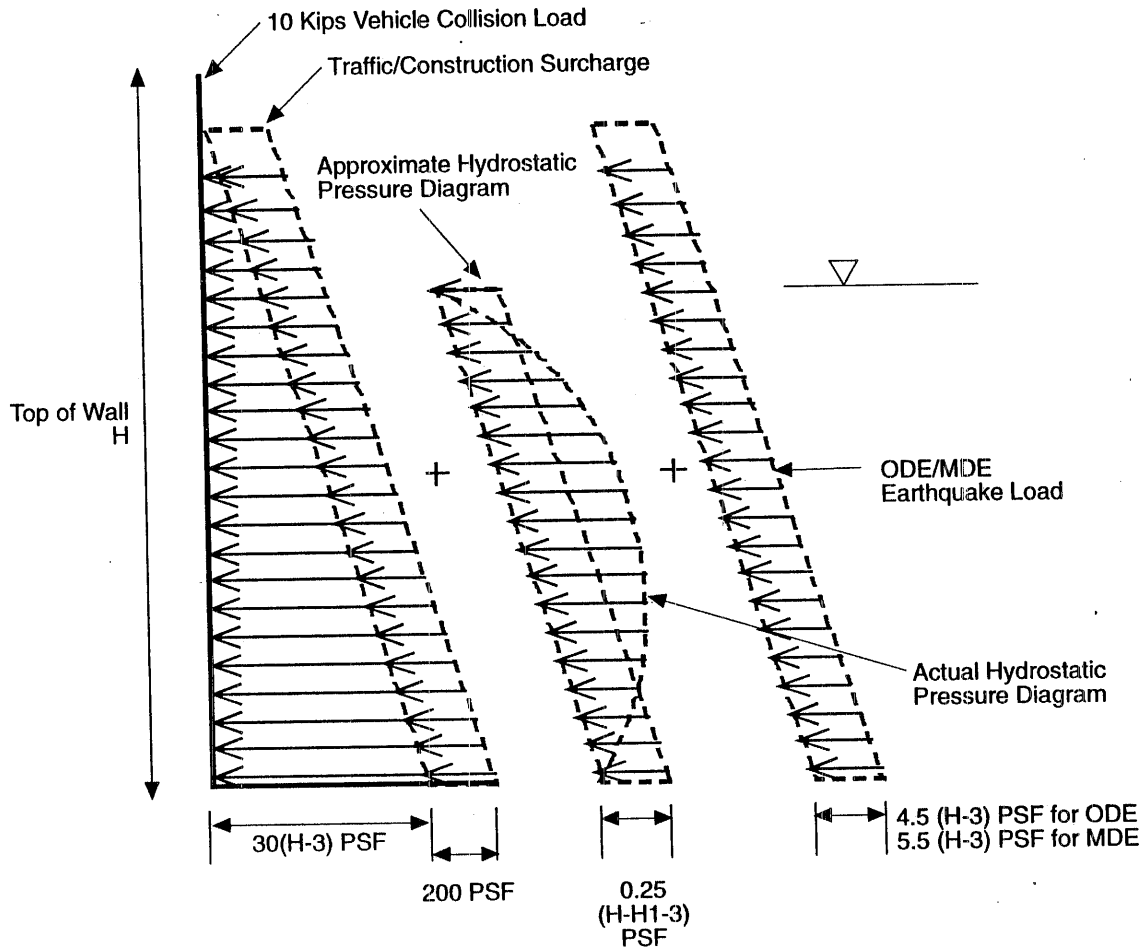

FIGURE **6**

DESIGN LATERAL EARTH PRESSURE

WALL 600/PRESENTATION/CO

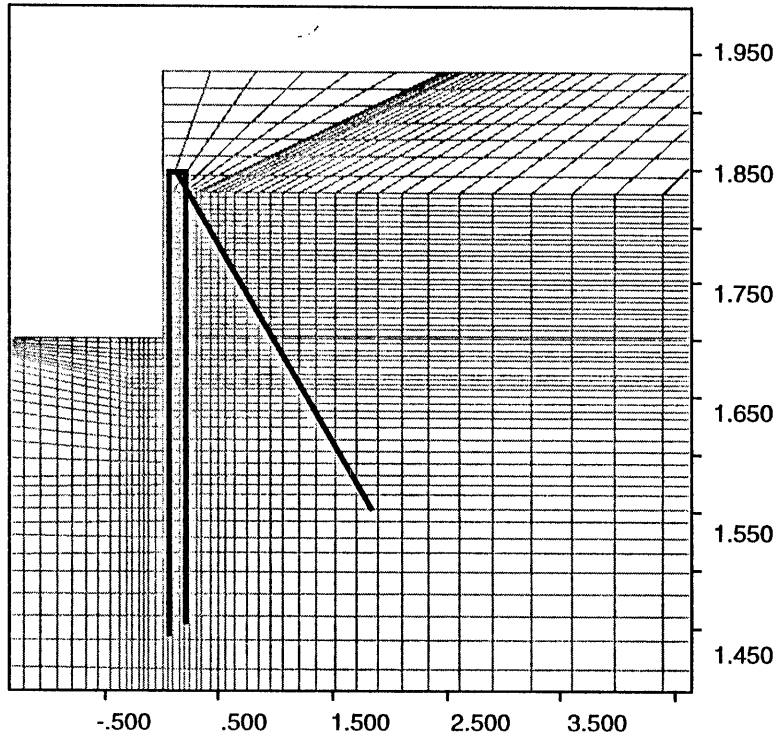

FIGURE 7
FINAL CONFIGURATION
FLAC MODEL
WALL 600/PRESENTATION/CO

PROJECT NO. IP3 2572 DRAWING NO. 66762 DATE 5/31/96 DRAWN BY EA

Golder Associates

Quantity Type	Structural Element	Quantity	Computed Values FLAC	STAAD-III
Force	Shotcrete Facing	Moment (k-ft/ft)	0.05	NA
		Shear (k/ft)	0.16	NA
	CIP Wall	Moment (k-ft/ft)	0.87	11.36
		Shear (k/ft)	1.72	3.02
	CIP Cantilever	Moment (k-ft/ft)	0.32	11.74
		Shear (k/ft)	0.11	3.02
	Outboard Micropile	Pipe Moment (k-ft)	16.99	47.70
		Pipe Shear (k)	23.48	8.05
		Bar Compression (k)	35.43	50.40
	Inboard Micropile	Pipe Moment (k-ft)	8.92	27.00
		Pipe Shear (k)	12.59	9.85
		Bar Compression (k)	47.58	27.20
	Inclined Micropile	Pipe Moment (k-ft)	5.43	32.03
		Pipe Shear (k)	2.42	9.85
		Bar Tension (k)	19.27	50.50
	Grade Beam	Moment (k-ft/ft)	4.89	21.07
		Shear (k/ft)	2.36	10.08
		Compression (k/ft)	2.57	3.62
Deflection	Horizontal	Top of Cantilever (in)	0.22	0.03
		Grade Beam (in)	0.46	0.16
		Maximum @ Wall (in)	0.92	0.22
		Wall Base (in)	0.47	0.05

FIGURE **8**
SUMMARY COMPARISION
FLAC AND STAAD III ANALYSIS MODELS
WALL 600/PRESENTATION/CO

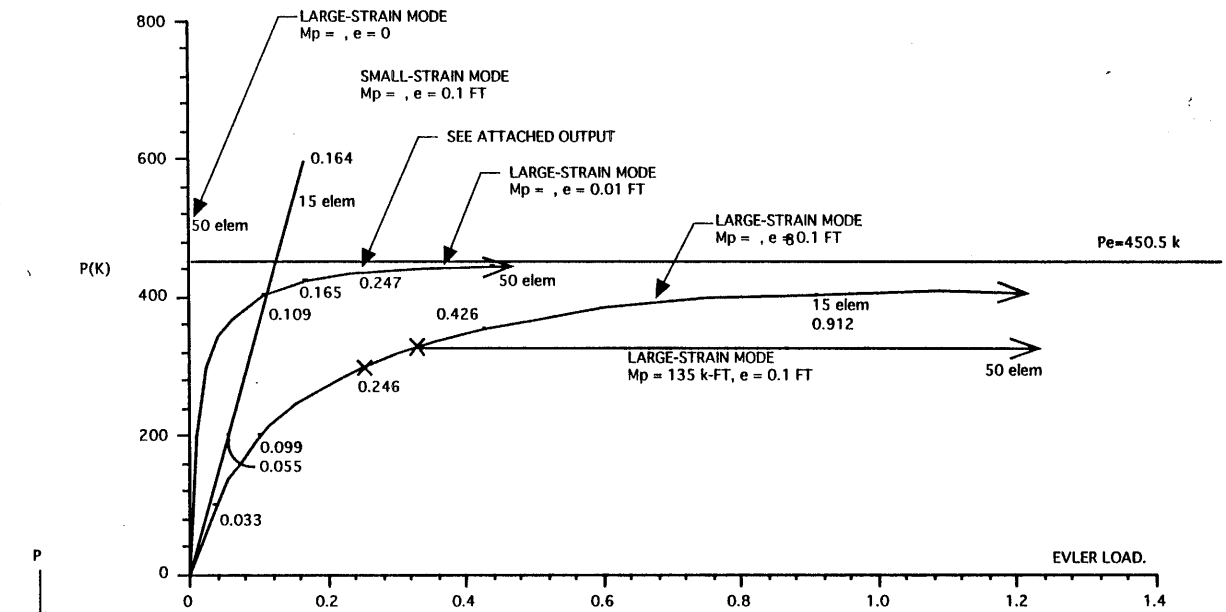

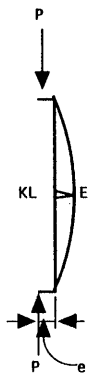

KL - 15 FT

e = ECCENTRICY OF LOAD P

7" DIA. (NOM) API MICROPILE
PIPE N80

Mp = 135 K-FT

FLAC ANALYSIS RESULTS

1. FOR SLIGHTEST ECCENTRICITY, FLAC PREDICTS BUCKLING AT EULER LOAD.

2. FOR LARGER ECCENTRICITY, BUCKLING LOAD DECREASES

3. PLASTIC MOMENT REDUCES BUCKLING LOAD EVEN MORE.

FIGURE **9**

SINGLE PILE AXIAL LOAD DEFLECTION RESPONSE

WALL 600/PRESENTATION/CO

PROJECT NO. IP3 2572 DRAWING NO. 66770 DATE 5/31/96 DRAWN BY EA

Golder Associates

INTERACTION DIAGRAM

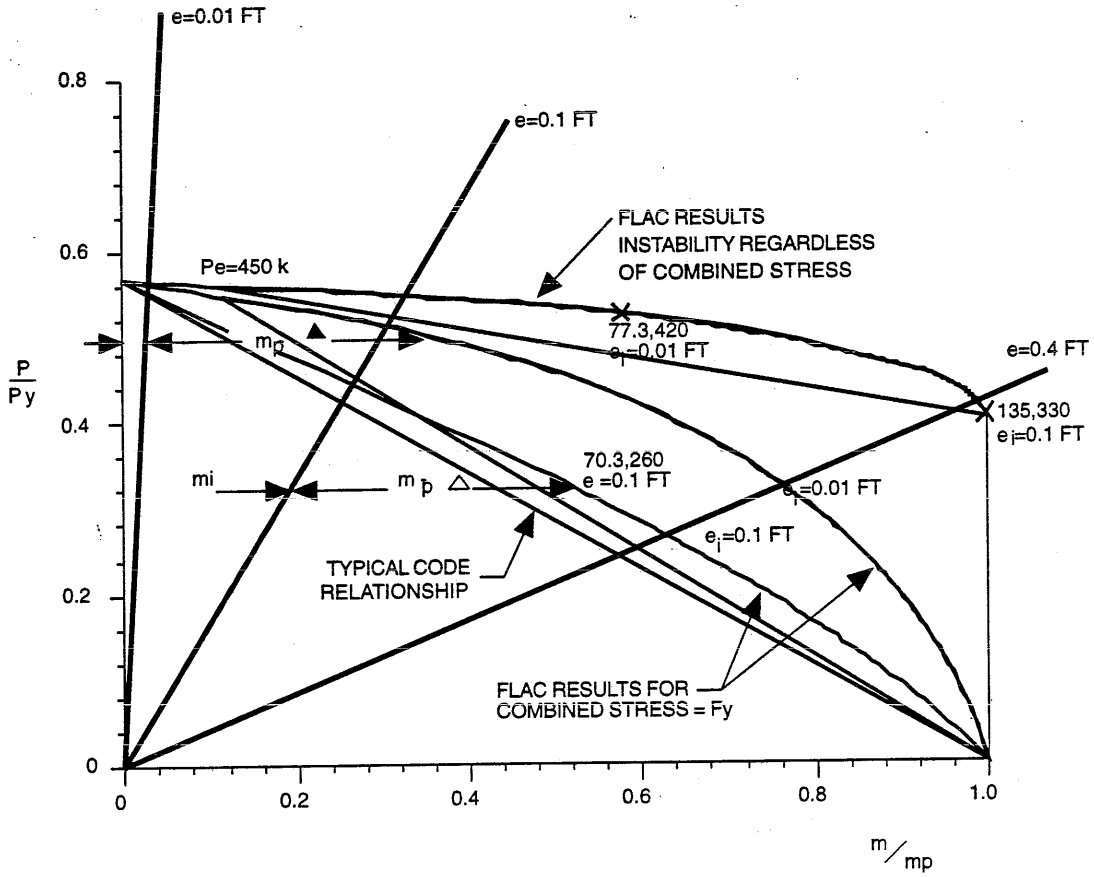

P = APPLIED AXIAL LOAD

M = MAXIMUM MOMENT

M = END MOMENT = P e_i

7" (NOM) DIA ATI N80 PIPE

KL = 15 FT i KL/r =

Py = 10(80) = 800 k (SHEET 1)

Pe = 450.5 (SHEET 1)

Mp = 135 k-FT (SHEET 1)

FIGURE **10**
INTERACTION DIAGRAM
WALL 600/PRESENTATION/CO

PROJECT NO. IP3 2572 DRAWING NO. 66769 DATE 5/31/96 DRAWN BY EA

Golder Associates

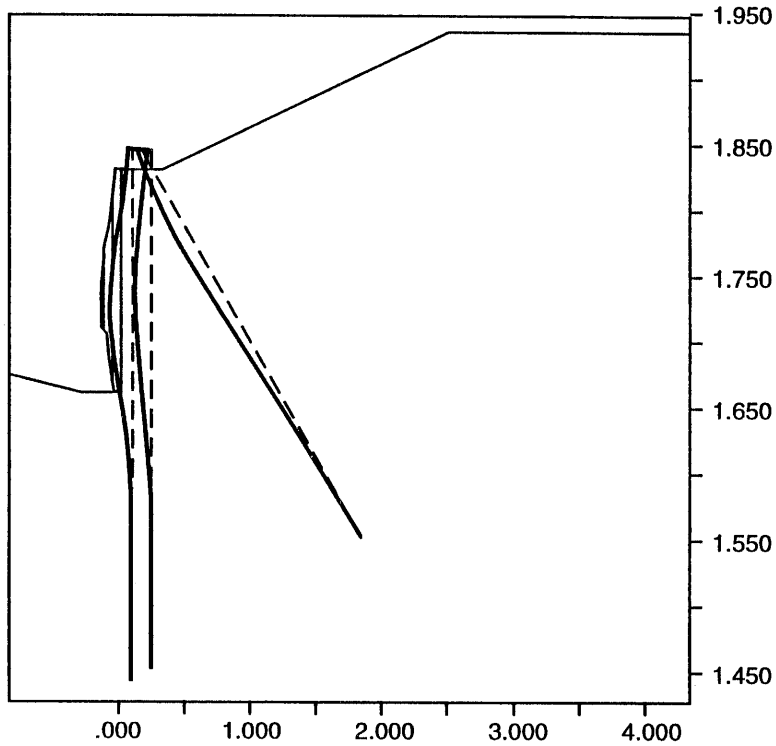

FIGURE **11**
STRUCTURAL DEFORMATION
END OF EXCAVATION
WALL 600/PRESENTATION/CO

PROJECT NO. IP3 2572 DRAWING NO. 66756 DATE 5/31/96 DRAWN BY EA

Golder Associates

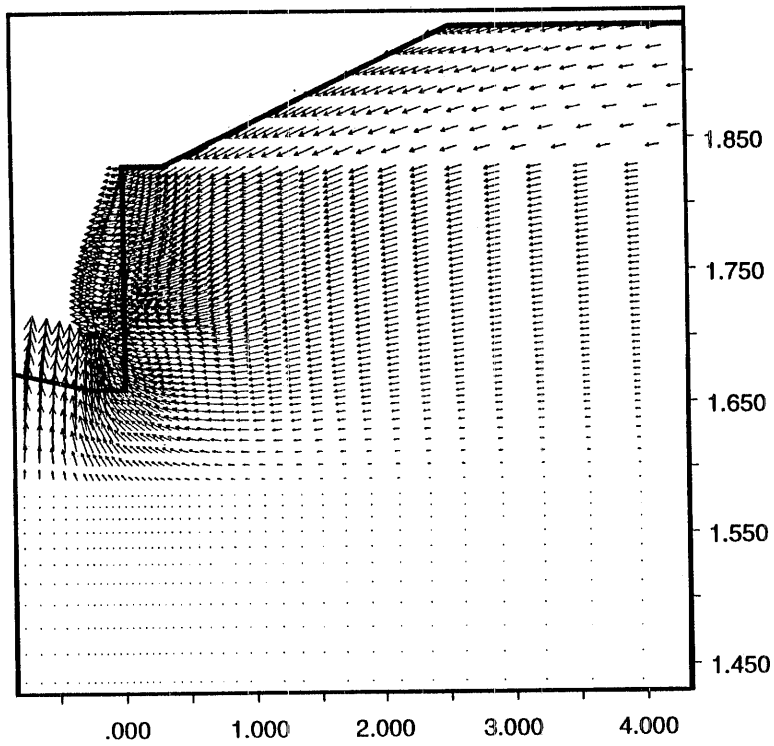

FIGURE **12**
DISPLACEMENT VECTORS
END OF EXCAVATION
WALL 600/PRESENTATION/CO

PROJECT NO. IP3 2572 DRAWING NO. 66751 DATE 5/31/96 DRAWN BY EA

Golder Associates

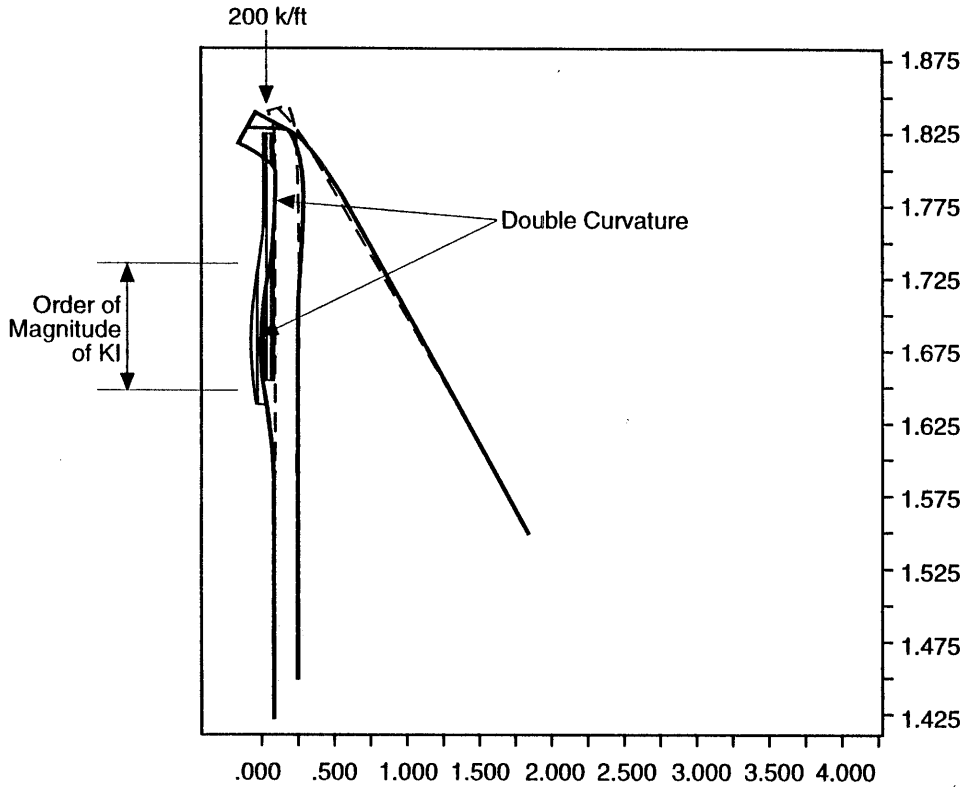

FIGURE **13**

STRUCTURAL DEFORMATION
END OF EXCAVATION WITH ARTIFICIAL LOAD
WALL 600/PRESENTATION/CO

PROJECT NO. IP3 2572 DRAWING NO. 66755 DATE 5/31/96 DRAWN BY EA

Golder Associates

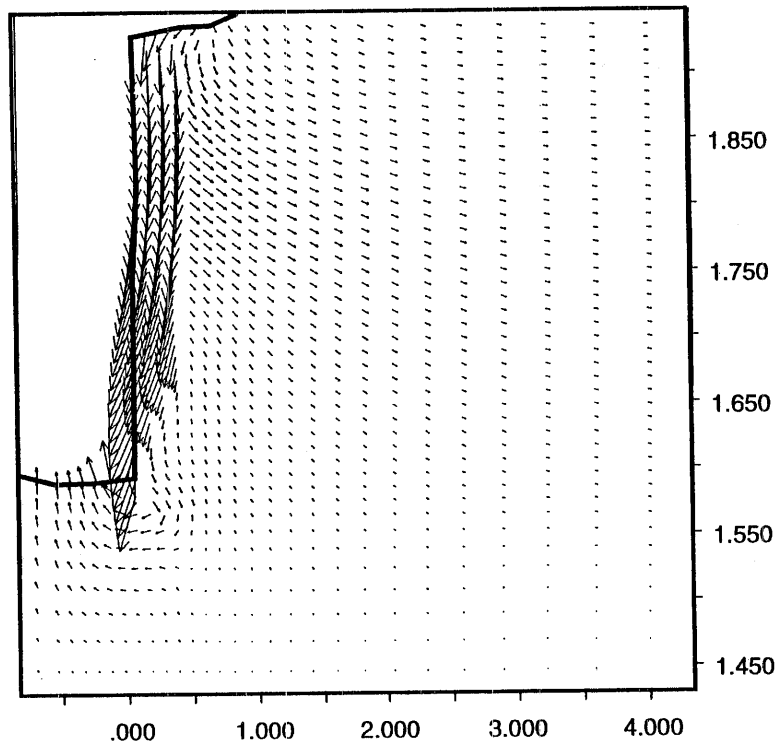

FIGURE 14
DISPLACEMENT VECTORS - END OF EXCAVATION, ARTIFICIAL LOADING
WALL 600/PRESENTATION/CO

PROJECT NO. IP3 2572 DRAWING NO. 66750 DATE 5/31/96 DRAWN BY EA

Golder Associates

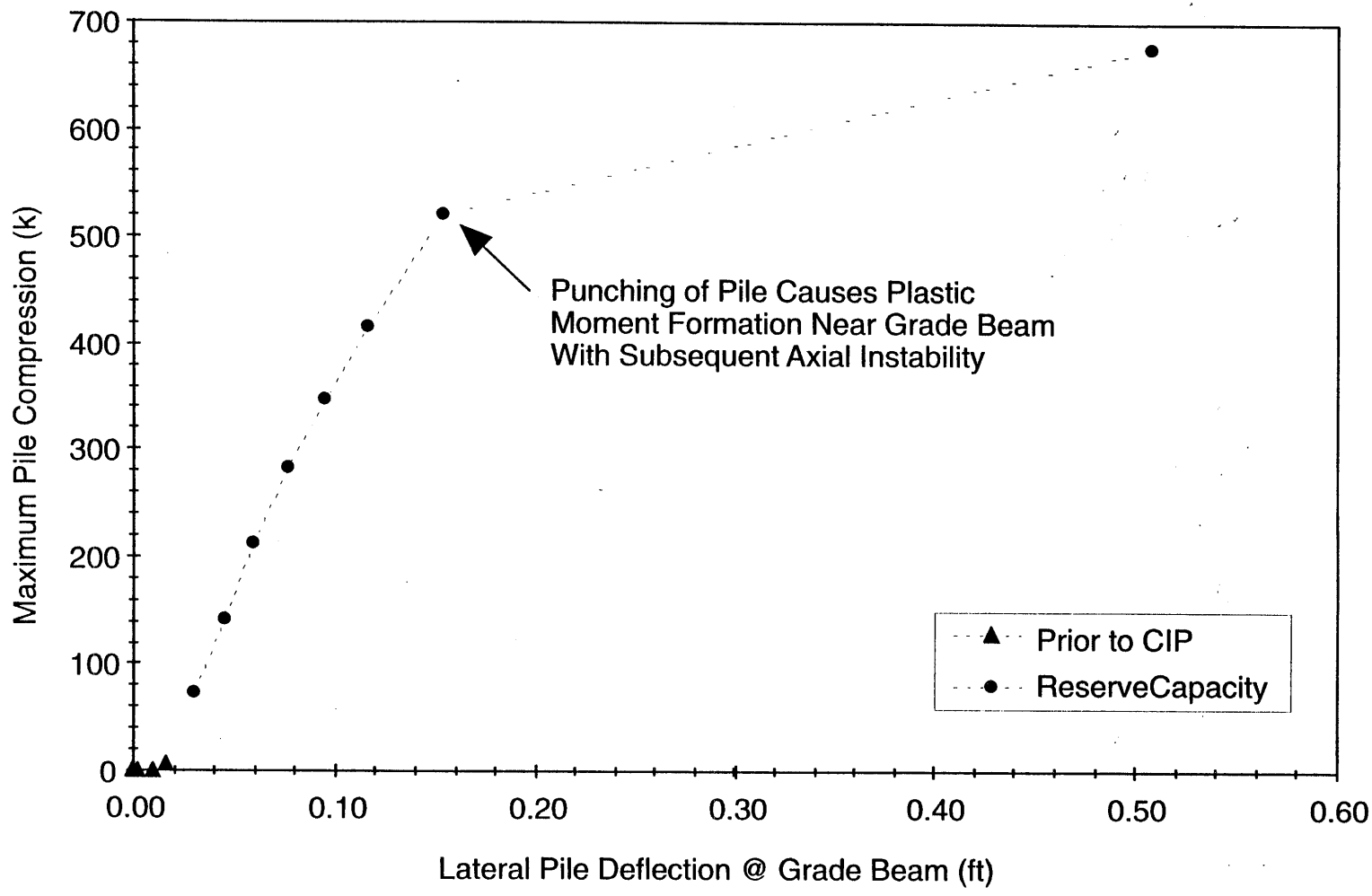

FIGURE **15**

FLAC RESULTS – END OF EXCAVATION
PILE 1 AXIAL LOAD LIMITS
WALL 600/PRESENTATION/CO

PROJECT NO. IP3 2572 DRAWING NO. 66765 DATE 5/31/96 DRAWN BY EA

Golder Associates

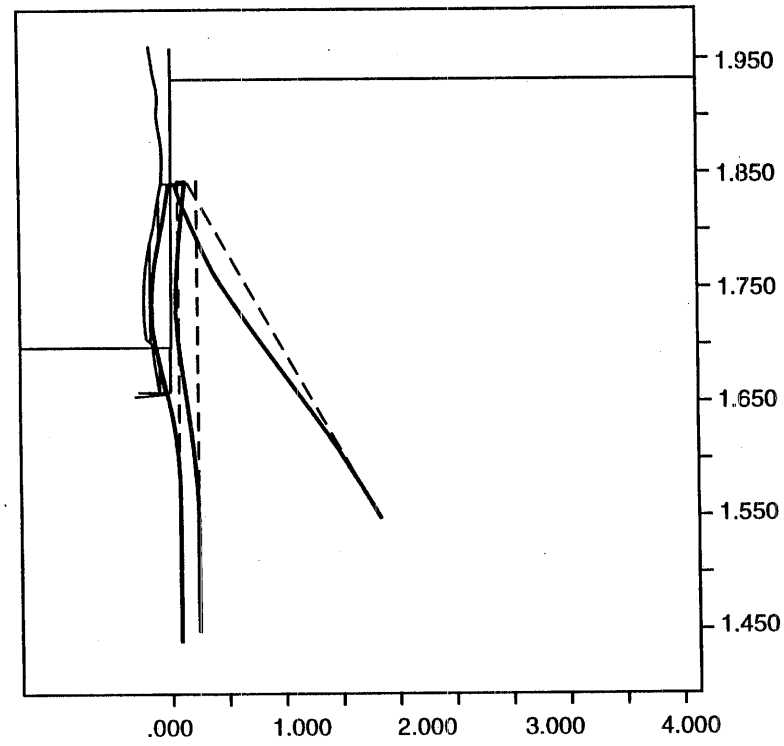

FIGURE **16**
STRUCTURAL DEFORMATION
FINAL CONFIGURATION
WALL 600/PRESENTATION/CO

PROJECT NO. IP3 2572 DRAWING NO. 66754 DATE 5/31/96 DRAWN BY EA

Golder Associates

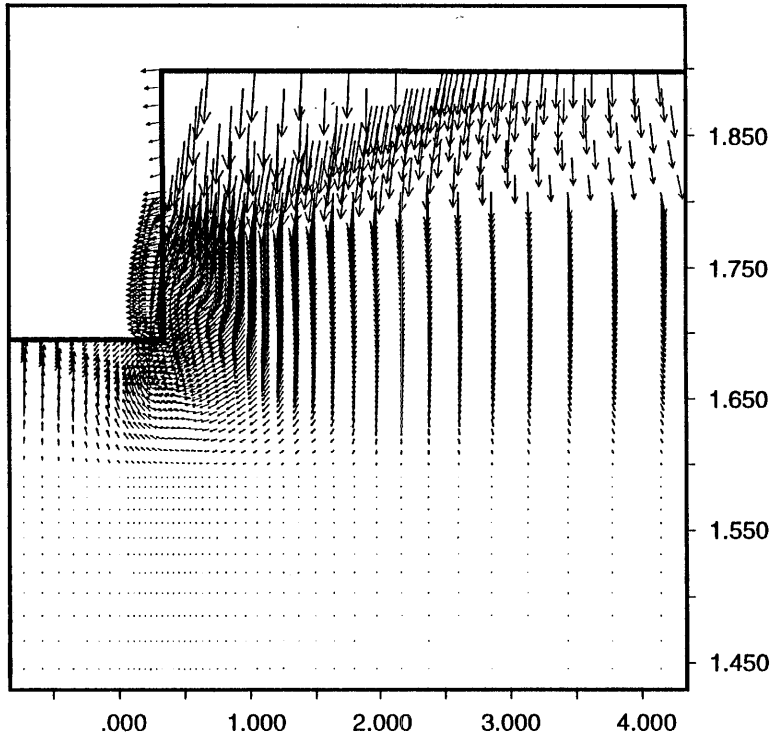

FIGURE **17**
DISPLACEMENT VECTORS
FINAL CONFIGURATION
WALL 600/PRESENTATION/CO

PROJECT NO. IP3 2572 DRAWING NO. 66752 DATE 5/31/96 DRAWN BY EA

Golder Associates

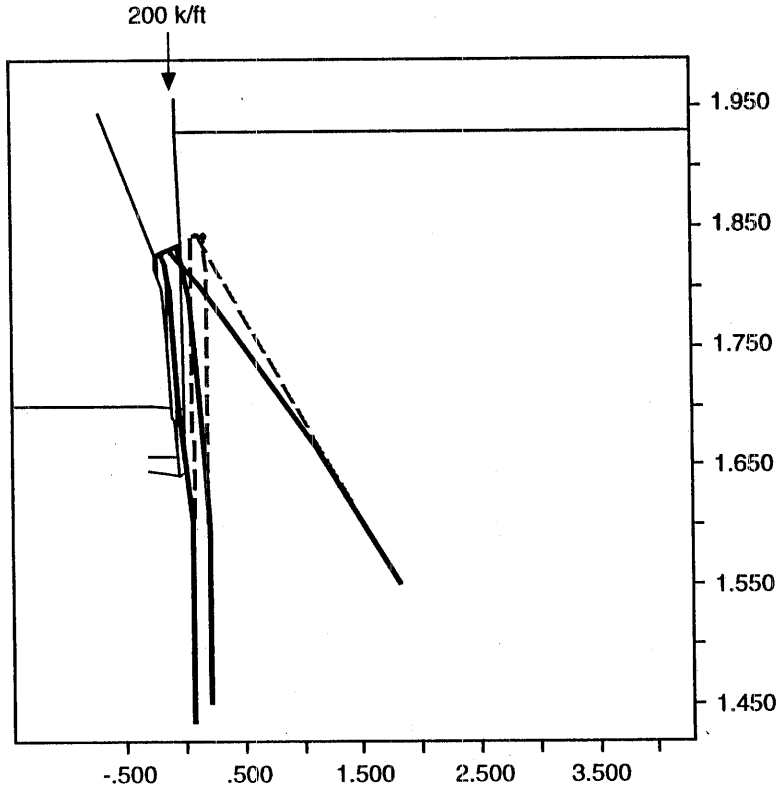

FIGURE **18**

STRUCTURAL DEFORMATION
FINAL CONFIGURATION WITH ARTIFICIAL LOAD
WALL 600/PRESENTATION/CO

PROJECT NO. IP3 2572 DRAWING NO. 66761 DATE 5/31/96 DRAWN BY EA

Golder Associates

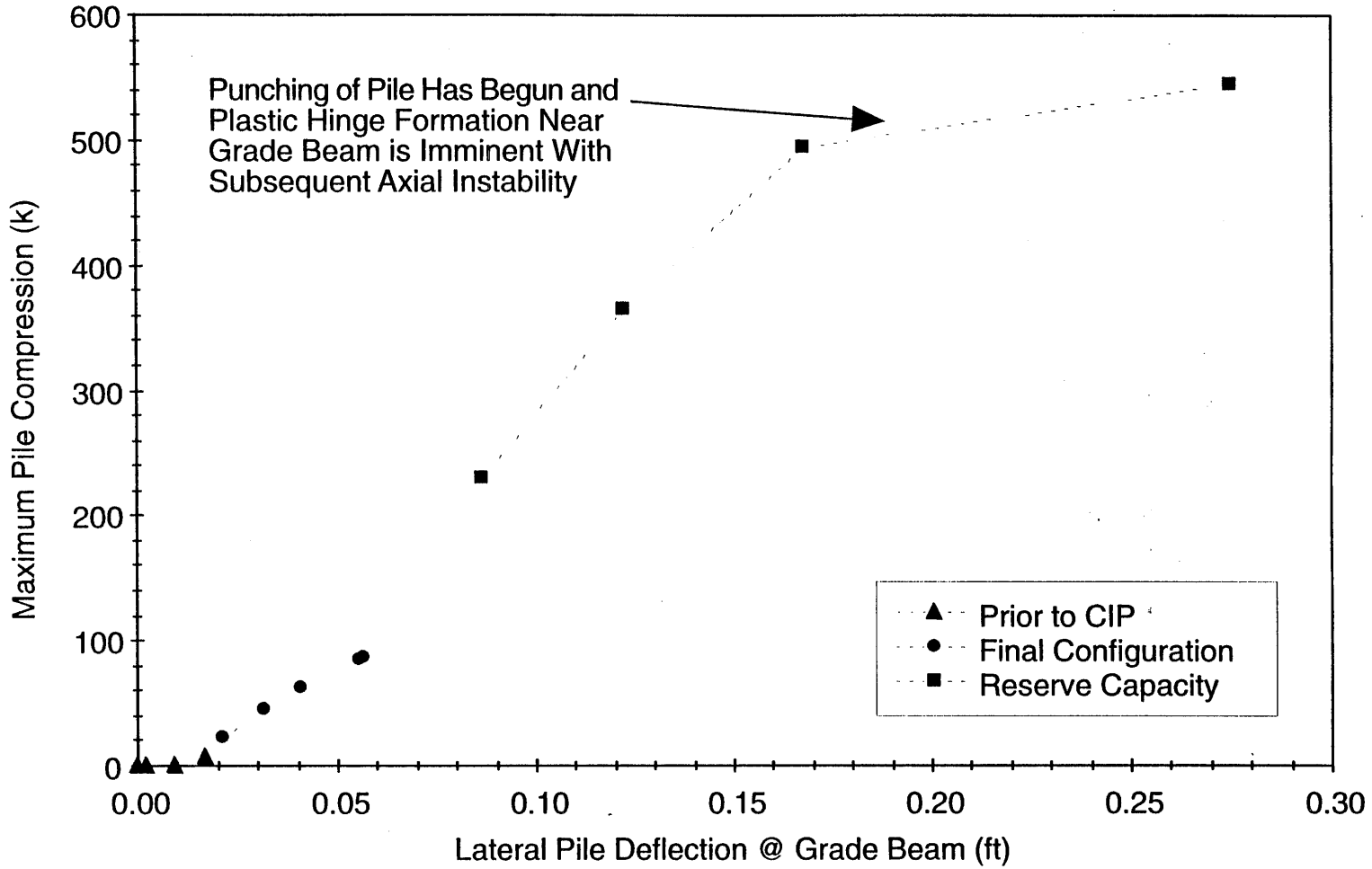

FIGURE **19**

FLAC RESULTS – FINAL CONFIGURATION
PILE 1 AXIAL LOAD LIMITS
WALL 600/PRESENTATION/CO

PROJECT NO. IP3 2572 DRAWING NO. 66766 DATE 5/31/96 DRAWN BY EA

Golder Associates

Stage	Externally Applied Axial Load (k/ft)	Externally Applied Axial Load Location	Pile 1 Maximum Axial Load P_U (k)	Pile 2 Maximum Axial Load P_U (k)	Pile 1 Maximum Moment M_U (k-ft)	Pile 2 Maximum Moment M_U (k-ft)	Pile 1 Grade Beam Lateral Deflection δ_{GB} (ft)	Pile 1 Maximum Lateral Deflection δ_{MAX} (ft)	Pile 1 Wall Base Lateral Deflection δ_{BASE} (ft)	Pile 1 P_U/P_Y	Pile 1 M_U/M_P	Pile 1 Total Ratio
Initialize	0.0	-	0.0	0.0	0.0	0.0	0.000	0.000	0.000	0.00	0.00	0.00
Excav Lift 1	0.0	-	0.0	3.7	8.4	3.5	0.002	0.004	0.005	0.00	0.06	0.06
Excav Lift 2	0.0	-	0.5	27.9	15.4	12.7	0.009	0.033	0.016	0.00	0.11	0.11
Excav Lift 3	0.0	-	6.7	59.5	22.6	19.4	0.017	0.085	0.047	0.01	0.17	0.18
Reserve A1	20.0	Pile 1	72.0	90.0	32.1	18.5	0.030	0.086	0.047	0.09	0.24	0.33
Reserve A3	60.0	Pile 1	211.5	151.5	48.8	31.1	0.059	0.085	0.046	0.26	0.36	0.62
Reserve A5	100.0	Pile 1	347.0	220.0	67.3	48.2	0.095	0.084	0.045	0.43	0.50	0.93
Reserve A7	150.0	Pile 1	521.0	316.0	96.6	73.6	0.154	0.084	0.047	0.65	0.71	1.36
Reserve A8	200.0	Pile 1	675.0	286.0	99.0	99.0	0.508	0.160	0.123	0.84	0.73	1.58
CIP & Fill 1	0.0	-	23.0	68.5	27.8	16.8	0.021	0.087	0.045	0.03	0.21	0.23
Fill 2	0.0	-	44.5	88.0	33.7	17.8	0.031	0.096	0.047	0.06	0.25	0.30
Fill 3	0.0	-	62.0	105.5	39.2	19.5	0.041	0.105	0.052	0.08	0.29	0.37
Surcharge	0.0	-	84.5	142.5	47.8	26.9	0.056	0.127	0.065	0.11	0.35	0.46
Impact	0.0	-	86.5	142.5	49.3	27.0	0.057	0.128	0.065	0.11	0.36	0.47
Reserve B1	50.0	Pile 1	229.8	224.5	64.1	23.6	0.086	0.127	0.063	0.29	0.47	0.76
Reserve B2	100.0	Pile 1	365.5	308.0	78.9	19.8	0.122	0.125	0.060	0.46	0.58	1.04
Reserve B3	150.0	Pile 1	494.0	399.5	96.7	27.2	0.168	0.126	0.055	0.62	0.71	1.33
Reserve B4	200.0	Pile 1	544.5	548.5	98.8	47.8	0.275	0.133	0.051	0.68	0.73	1.41
Reserve B3	200.0	Middle	531.5	555.0	41.6	33.6	0.202	0.235	0.088	0.66	0.31	0.97
Reserve B4	250.0	Middle	638.5	547.5	99.0	98.9	0.720	0.837	0.233	0.80	0.73	1.53

Py = 800 K
Mp = 135.3 k ft

FIGURE **20**
SUMMARY OF FLAC INTERACTION ANALYSES
WALL 600/PRESENTATION/CO

PROJECT NO. IP3 2572 DRAWING NO. 66764 DATE 5/31/96 DRAWN BY EA

Golder Associates